

CONFIDENTIAL

Copy  
RM E53L24

6

NACA RM E53L24



# RESEARCH MEMORANDUM

INVESTIGATION OF A SUPERSONIC-COMPRESSOR ROTOR  
WITH TURNING TO AXIAL DIRECTION  
II - ROTOR COMPONENT OFF-DESIGN  
AND STAGE PERFORMANCE

By Melvin J. Hartmann and Edward R. Tysl

Lewis Flight Propulsion Laboratory  
Cleveland, Ohio

CLASSIFICATION CHANGED

UNCLASSIFIED

To \_\_\_\_\_

By authority of NACA Research  
FRN-124 Date Jan 20, 1958  
AM-2-12-58

CLASSIFIED DOCUMENT

This material contains information affecting the National Defense of the United States within the meaning of the espionage laws, Title 18, U.S.C., Secs. 793 and 794, the transmission or revelation of which in any manner to an unauthorized person is prohibited by law.

**NATIONAL ADVISORY COMMITTEE  
FOR AERONAUTICS**

WASHINGTON

March 12, 1954

**LIBRARY COPY**

LANGLEY RESEARCH LABORATORY  
1936  
LANGLEY FIELD, VIRGINIA

CONFIDENTIAL



## NATIONAL ADVISORY COMMITTEE FOR AERONAUTICS

RESEARCH MEMORANDUMINVESTIGATION OF A SUPERSONIC-COMPRESSOR ROTOR WITH TURNING TO AXIAL  
DIRECTION. II - ROTOR COMPONENT OFF-DESIGN AND STAGE PERFORMANCE

By Melvin J. Hartmann and Edward R. Tysl

## SUMMARY

The aerodynamic design and the design-point performance of a 16-inch impulse-type supersonic-compressor rotor component with turning to the axial direction were investigated in part I of this series. The possibility of good stage performance was indicated; therefore, in this report the off-design and the stage performance are analyzed. The analysis of the stage performance was made with a set of diffusing stators designed from considerations of the off-design performance.

The characteristics of this rotor were such that the rotor-discharge Mach number could be reduced from that obtained at the design condition of 1.94 to about 1.65 without a large drop in performance. But closing the throttle farther to reduce the discharge Mach number resulted in a considerable decrease in rotor component performance. This rotor characteristic resulted in the peaking of computed stage performance at an intermediate Mach number (about 1.55) when the stator losses were assumed similar to those previously obtained. Thus, the computed best stage-performance point is obtained at this intermediate rotor-discharge Mach number rather than at the design condition for the rotor. The computed stage-performance curves indicate the rather critical nature of the matching problem between the rotor and stator performance characteristics and the possibility of improving the stage performance by decreasing the losses in the diffusing stators.

The stators set at the design angle limited the rotor operation at 97.5-percent design speed to a point below the best computed stage-performance point. Under these conditions, the stage total-pressure ratio was about 4.0 and the stage adiabatic efficiency was about 0.66. Reducing the stator angle  $6^\circ$  below the design angle increased the stage performance at 77.9-percent design speed from a total-pressure ratio of 2.5 to 2.7 and from an adiabatic efficiency of 0.70 to 0.77. This increase was a result of improved rotor performance and also improved stator total-pressure recoveries. The reduction in stator angle improved stator total-pressure recoveries at Mach numbers below 1.25 but

seemed to have little effect on the total-pressure recoveries above this value. These stator recoveries are slightly higher than those obtained in the previous stator investigation.

## INTRODUCTION

Impulse-type supersonic-compressor rotors are designed to impart energy to the fluid by a large amount of turning with a relatively small amount of diffusion (static-pressure rise) in the rotor passage. In these design configurations, the flow relative to both the rotor blade row and the diffusing stators is supersonic. Considerable deceleration is then required in the stators to obtain useful flow velocities. Several compressor rotors of this type have been experimentally investigated and are reported in references 1 to 4. In references 1 to 3, impulse-type supersonic-compressor rotor component total-pressure ratios of 3.6 and 6.6 were obtained at adiabatic efficiencies of 0.80 and 0.78, respectively. In reference 4 (part I of this series) a total-pressure ratio of 5.7 was reported at an adiabatic efficiency of about 0.89.

The compressor rotor of reference 4 represents a considerable improvement over previous rotors for design, or impulse, operation. Also, there was only a moderate drop in efficiency with reduced discharge Mach numbers (i.e., increased back pressure). This contrasted markedly with previous impulse-type compressor rotors, where appreciable reductions in efficiency were observed with increased back pressure. These characteristics are attractive with respect to the use of this rotor with diffusing stators as a stage. Before a satisfactory stage can be designed, the problems associated with diffusing stators must be considered.

References 3 and 5 indicate that the losses in diffusing stators increase very rapidly with stator-entrance (rotor absolute discharge) Mach number. (For the rotor of ref. 4 the design absolute discharge Mach number is about 1.93.) However, as stated previously, the rotor of reference 4 operated at somewhat reduced Mach numbers without a large drop in performance. The reduced losses in the stators, arising from operation at the lower entrance Mach number obtainable by increasing the back pressure on the rotor, appear to more than offset the slight drop in rotor performance. Consequently, the optimum combination for operation with stators may occur with the rotor operating at an off-design condition. This report presents the more complete analysis of the off-design performance of the compressor rotor that was a necessary preliminary in determining the rotor operational point for the best stage performance. The stage performance was then analytically determined with the assumption of the stator recoveries obtained in a previous stator investigation (ref. 3). After these considerations, a desirable rotor operational point was selected for the design of diffusing stators, with particular attention given to the flow area. Performance data obtained for the stage and the stators at the design setting angle as well as at 3° and 6° below design are included in this report. The data were obtained at the NACA Lewis laboratory; Freon-12 was used as the test medium.

## APPARATUS

## Impulse-Type Supersonic-Compressor Rotor

A photograph of the 16-inch impulse-type supersonic-compressor rotor with turning to the axial direction is shown in figure 1(a). This rotor was designed by a quasi-three-dimensional design procedure that permitted good mechanical design. The design procedure is described in detail in reference 4.

## Diffusing Stators

The stators were designed to allow sufficient area so that they would not restrict the rotor weight flow. The flow-area considerations included an allowance for losses by noting that the change in critical flow area is dependent on the losses by

$$\frac{A_a^*}{A_b^*} = \frac{P_b}{P_a} \quad (1)$$

where  $A^*$  is the critical flow area;  $P$  is the total pressure;  $a$  is the upstream condition; and  $b$  is the minimum-area section. The change in area from the upstream condition to the minimum section is defined as the contraction ratio  $Cr$ , or

$$Cr = \frac{A_a}{A_b} \quad (2)$$

where  $A$  is the flow area.

Equations (1) and (2) can be combined by

$$Cr = \frac{A_a^*/A_b^*}{A_a^*/A_a} = \frac{(A_b^*/A_b)(P_b/P_a)}{A_a^*/A_a}$$

and, if the minimum section  $b$  is designed to have a Mach number of 1.0 ( $A_b^*/A_b = 1.0$ ):

$$Cr = \frac{P_b/P_a}{A_a^*/A_a} \quad (3)$$

A point was selected at 97.5-percent design speed of the rotor at which the stator-inlet Mach number was about 1.55 and the flow angle was about  $57.4^\circ$ . (The reason for the selection of this design point will be discussed in the off-design analysis of the data for the compressor rotor component.) By setting  $P_b/P_a$  at a value near normal shock losses at this Mach number,  $C_r$  was determined to be about 1.11. With this contraction ratio and the preceding allowance for losses, the area at the minimum section was found to be suitable to allow the rotor to operate at its maximum weight-flow point at all speeds above about 70-percent design speed.

The blading was designed so that the minimum-area section occurred at the entrance to the stator passage, with a constant area for a distance equal to the passage width. The number of stator blades was set at 31; flow direction at the minimum-area section was set equal to the entrance flow direction; area increase behind the minimum section was set equivalent to a  $5^\circ$  cone with an initial area equal to the minimum area; and exit flow direction was set at  $47^\circ$ , and trailing-edge thickness at 0.03 inch. The length of the subsonic portion of the blade was then computed to be 1.7 inches to obtain the desired change in area along a straight circular cone. Thus, with these specifications, the minimum area, the blade length, and the flow direction at the entrance, minimum-area, and exit sections were fixed. The blade surfaces were faired to meet these requirements. This blade section was used at the root and tip sections, with straight-line fairing between these two sections and a  $5^\circ$  twist from root to tip. The leading-edge wedge angle was about  $10^\circ$  and was rounded to a leading-edge thickness of 0.015 inch. The design setting resulted in a suction-surface angle of about  $64.3^\circ$  and a pressure-surface angle of about  $54.3^\circ$  at the mean-radius section. A photograph of the stators is shown in figure 2.

#### Variable-Component Test Rig

The data used in this analysis were obtained with the rotor installed in the variable-component compressor test rig adapted to use Freon-12 as the testing medium. This test rig is shown schematically in figure 1(b) and is described in detail in reference 4. The rotor component data were obtained with both a straight- and an expanding-discharge annulus (see fig. 1(b) and ref. 4). The diffusing stators used in the stage investigation were installed in the straight-discharge annulus about  $2\frac{1}{8}$  inches behind the compressor rotor.

#### Instrumentation

The rotor component data with the expanding-discharge annulus were obtained with instrumentation at station 2 (fig. 1(b)). A cone-type

survey instrument was used to measure total pressure and flow direction, and total temperature was obtained with a double-stagnation-type probe; inside and outside wall taps were used to obtain the static pressure (ref. 4). The survey instruments were slightly different for the straight-discharge-annulus data, in that a claw-type total-pressure instrument was used to determine the flow angle and total pressure at station 2, and the total temperature was obtained from a stagnation-type thermocouple. A photograph of these survey probes is shown in figure 3.

The stage data were obtained at station 3 (fig. 1(b)), 0.5 inch behind the stators. The previously described flow-angle and temperature probes were used at this instrument station along with a 24-tube total-pressure survey rake (fig. 3). The 24 total-pressure tubes on this rake, which were equally spaced and sufficient to cover approximately one stator passage, were inclined to the mean-radius section and mean blade angle. The rake was rotated to the flow direction according to a claw-total survey instrument at this survey station. Static pressures at the survey stations were averaged from several taps on the inside and outside walls.

In order to keep the closed Freon-12 circuit as small as possible, the entrance nozzle to the compressor was calibrated to determine the flow rate through the compressor. Fixed probes in the entrance tank determined the total pressure and temperature at this location (station 0).

## PROCEDURE

### Operational Procedure

The compressor rotor component was operated in Freon-12 over a range of speeds from 48.7 to 97.5 percent of design. The design rotor speed in Freon-12 was computed so that the design relative entrance Mach number would be obtained at the rotor tip. The inlet temperature was maintained constant at  $100^{\circ} \pm 1.0^{\circ}$  F and the inlet pressure at  $30.0 \pm 0.1$  inches of mercury absolute by the automatic controls of the test rig. The back pressure was varied from the open-throttle condition to audible surge by the sliding throttle installed in the collector (fig. 1(b)).

The rotor component data included in part I of this series (ref. 4) were obtained with a discharge annulus of increasing area, which allowed the rotor to operate near its design condition. These data are included in the present analysis along with the data obtained with the straight-discharge annulus. The stage investigation was made with the impulse rotor and diffusing stators previously described installed in the straight-discharge annulus.

### Computational Procedure

The compressor rotor performance data are based on the flow conditions measured in the depression tank and the survey data obtained directly behind the rotor (station 2). Stage performance was obtained from measurements in the depression tank and at station 3. The total pressures obtained from the 24-tube total-pressure rake at station 3 were averaged arithmetically at each survey position and mass-averaged along the radius. The computational procedure is described in appendix B of reference 1 for experimental data obtained in Freon-12. An approximate air equivalent weight flow can be obtained by the methods described therein.

The consistency of the data at design conditions was indicated in reference 4, where the change in angular-momentum work input agreed with the measured temperature-rise work input within about 2 percent, and the measured electrical power varied from the measured temperature-rise work input by 4 percent. The survey data at station 2 indicate a weight flow 1.6 percent greater than that measured by the inlet calibrated nozzle. This agreement is typical of all open-throttle data. As the back pressure is applied, the absolute discharge Mach number remains supersonic, but the axial component becomes subsonic. This change results in substantial disagreement in the previously mentioned terms, probably largely as a result of erroneous angle measurements. In general, total pressure, total temperature, wall static pressure, and nozzle weight flow are considered essentially correct and are used in this report. (The calibrated nozzle is relatively close to the rotor; however, static-pressure profiles along the outside wall indicate that the rotor does not measurably affect the nozzle calibration.)

### RESULTS AND DISCUSSION

Examination of the limited amount of data presented in reference 4 and some preliminary data indicates that good stage performance might be obtained by operating this impulse-type rotor at a reduced flow point. At this point, the rotor absolute discharge Mach number decreased considerably with respect to the design value, with only a small reduction in rotor efficiency and total-pressure ratio. Before the best rotor and stator matching point could be determined, however, it was necessary to analyze the rotor component performance over the entire weight-flow range.

#### Rotor Component Performance

Rotor over-all performance. - The data of reference 4 were obtained with an expanding annulus behind the rotor, with which operation near

design impulse was possible. With this expanding annulus, there were only small reductions in total-pressure ratio and equivalent weight flow between the open-throttle point and audible surge. The data of reference 4 and those obtained with the straight-discharge annulus are both shown in figures 4 to 7 (the solid symbols represent data obtained for the constant-area annulus). A much wider range of equivalent weight flow was obtained when the straight-discharge annulus was used; however, this increased range was at the low-weight-flow end of the performance curve, and impulse operation could not be obtained (fig. 4(a)). The fact that impulse operation is not possible must be due to choked flow resulting from losses in the discharge annulus. At 97.5-percent design speed, a peak total-pressure ratio of 5.7 is obtained at an equivalent weight flow of 48.55 pounds per second of Freon-12; a minimum pressure ratio is obtained at an equivalent weight flow of 41.5 pounds per second. Closing the discharge throttle farther results in decreasing weight flow and increasing total-pressure ratio. The curve obtained at 87.6-percent design speed shows a similar trend. Continuously decreasing performance values are obtained at the lower rotational speeds.

The variation of adiabatic efficiency for this rotor is shown in figure 4(b). At 97.5-percent design speed, a peak adiabatic efficiency of 0.89 is obtained. As the discharge throttle is closed, the adiabatic efficiency is reduced a few percentage points at constant weight flow. As the weight flow is decreased, the efficiency falls off rapidly. A minimum efficiency of about 0.71 is obtained at 40.0 pounds per second equivalent weight flow. Closing the discharge throttle to the point of audible stall results in a reduction in weight flow to about 34.2 pounds per second and an increase in adiabatic efficiency to about 0.745. Thus, the variation of adiabatic efficiency is very similar to the variation of total-pressure ratio. At lower rotational speeds, the peak adiabatic efficiency remains high at or near the open-throttle condition. However, closing the discharge throttle to the point of audible stall results in a large drop in adiabatic efficiency. Some scatter in the data occurs at the lower-weight-flow end of the curves at the lower rotational speeds.

The variation of mass-averaged absolute discharge Mach number at each of the six rotational speeds used in this investigation is shown in figure 4(c). The data at 97.5-percent design speed indicate a rapid drop in Mach number from 1.93 to about 1.63 with a change in total-pressure ratio of only 5.7 to 5.5. However, as the Mach number is decreased from 1.63 to about 1.40, the total-pressure ratio decreases much more rapidly to a value of 4.60, the minimum total-pressure ratio and Mach number occurring at the same point. As the throttle is closed farther, the Mach number and total-pressure ratio both increase. The fact that these data double back along the same curve is a result of the use of mass-averaged values of total-pressure ratio and absolute discharge Mach number. The data at other rotational speeds indicate similar curves of absolute discharge Mach number.

The adiabatic efficiency is plotted against the mass-averaged absolute discharge Mach number in figure 4(d). The variation in efficiency at design speed is similar to the variation in total-pressure ratio, decreasing gradually from about 0.89 at an absolute discharge Mach number of 1.93 to 0.85 at an absolute discharge Mach number of 1.65. As the absolute discharge Mach number is decreased further, the decrease in adiabatic efficiency is much more rapid to a value of about 0.71 at an absolute discharge Mach number of about 1.40. Similar curves are obtained at each speed, with a slight variation in the value of peak efficiency, and the lower speeds moving progressively to lower Mach numbers. A doubling back of data points similar to that noted in figure 4(c) occurs in figure 4(d).

Static-pressure profiles over rotor. - The static-pressure profiles over the compressor rotor for several of the data points at 97.5-percent design speed are shown in figure 5. The equivalent weight flow and mass-averaged absolute discharge Mach number are given for each data point. For the impulse condition ( $M_2 = 1.93$ ), the static pressure rises over about the first 20 percent of the rotor and remains constant over the rest of the rotor. As the back pressure is increased (Mach number decreased) the static-pressure rise over the rotor increases appreciably, occurring from the leading edge back over most of the rotor. At the minimum Mach number ( $M_2 = 1.40$ ,  $W\sqrt{\theta}/\delta = 42.5$  lb/sec), the static pressure ahead of the rotor is not affected; however, the maximum static-pressure rise is obtained at this point. Closing the throttle farther causes a considerable reduction in weight flow but an increase in discharge Mach number, with a resulting substantial static-pressure rise ahead of the rotor and a lower static-pressure rise over the rotor.

Performance measurements along rotor-discharge radius. - The radial variation of performance parameters at the rotor discharge at 97.5-percent design speed is shown in figure 6. At the impulse condition, the total-pressure ratio peaks near the hub portion of the rotor passage and decreases toward the tip. As the throttle is closed, the total-pressure ratio peaks (at a lower value) near the tip section and decreases toward the hub. The data point at the lowest weight flow indicates that the increase in pressure ratio over the previous point is obtained largely over the midpassage and tip regions.

For the impulse or open-throttle condition, the adiabatic efficiency (fig. 6) is very high (0.98) near the hub but decreases rapidly toward the tip (to about 0.80). The main effect as the discharge throttle is closed is a large decrease in adiabatic efficiency near the hub; whereas, the variation in efficiency at the tip section is appreciably less. At the lowest weight-flow point shown in figure 6, the adiabatic efficiency increases as indicated in figure 4(b).

The distribution of absolute discharge Mach number for these data points at 97.5-percent design speed varies in a manner similar to the total-pressure-ratio and adiabatic-efficiency distributions, the largest change in absolute discharge Mach number occurring at the rotor hub (fig. 6). The unit weight flow, however, has a somewhat different trend, in that it continues to decrease as the discharge throttle is closed. The largest unit weight flow is obtained near the tip section, with the slope of the unit mass-flow curve increasing as the discharge throttle is closed. The enthalpy rise over the rotor is larger at the tip than at the rotor hub section for the impulse condition, as indicated in figure 6. As the discharge throttle is closed, the work input at the tip section increases; whereas, the work input at the hub section remains nearly constant.

#### Discussion of Rotor Performance

If an impulse-type supersonic-compressor rotor is to perform at the design condition, the discharge annulus must not limit the weight flow. In reference 4, it was necessary to use an expanding-discharge annulus to obtain the design condition. (This was not necessary in the case of similar rotors reported in the references of this report.) Since these compressor rotors operate with supersonic relative velocities, a change in static-pressure rise over the rotor does not result in a change in weight flow until the static-pressure rise has propagated upstream to affect the subsonic axial upstream flow. Audible stall may occur before propagation of this static-pressure rise can be felt upstream and thus prevent the rotor from operating at reduced weight flows. Some of the rotors of this type reported in the references have operated with reduced weight flows; whereas, others have indicated audible stall before any noticeable reduction of weight flow was obtained. It was noted that changing the discharge annulus had a considerable effect on the point of audible stall of this compressor rotor.

With the previously mentioned considerations, the measured performance characteristics of this compressor rotor can be examined. As diffusion is first obtained in the compressor rotor, there is a small decrease in adiabatic efficiency and total-pressure ratio with no measurable change in equivalent weight flow. With the first measurable change in equivalent weight flow, a slight static-pressure rise is noted at the leading edge of the rotor. As additional diffusion (static-pressure rise) is obtained on the rotor, the total-pressure ratio, adiabatic efficiency, and equivalent weight flow all decrease rapidly. These changes in performance are obtained with an increasing static-pressure rise at the leading edge of the rotor; however, this static-pressure rise does not propagate very far upstream of the rotor (fig. 5). Near the point of audible stall, however, the static-pressure rise is apparently felt some distance upstream of the rotor and results in an increase in total-pressure ratio and adiabatic efficiency and a considerable reduction in equivalent weight flow.

These decreases in compressor performance appear to result mainly from deterioration of the flow near the compressor hub section. Increasing the diffusion over the rotor resulted in a definite decrease in total-pressure ratio and adiabatic efficiency at the rotor hub section from their values measured at the open-throttle condition, whereas the change in performance at the tip section is comparatively small. The mass-flow distribution at the compressor rotor discharge at the points of high diffusion on the rotor (near audible stall) indicates that a larger percentage of the mass flow is present at the rotor tip section. While this redistribution of the flow toward the tip section at low weight flows may have been caused by flow separation along the rotor hub, the mass distribution at the discharge could not be measured close enough to the hub section to determine whether the flow separation existed at the rotor discharge.

The supersonic-compressor rotor of this investigation was designed with turning to the axial direction. Thus, for ideal flow, operation with diffusion on the rotor would not change the work input to the fluid, since the absolute discharge whirl will be very nearly equal to the wheel speed at all times. For this reason, the total-pressure ratio and the adiabatic efficiency of the compressor rotor at a fixed wheel speed and radius would vary only as the losses on the rotor. In this case, however, (with no inlet whirl component) there is some variation in work input along the rotor-discharge radius. Therefore, a redistribution of the mass flow at the rotor discharge may result in some change in the mass-averaged performance.

Thus, a part of the performance characteristics (that is, the increasing total-pressure ratio and adiabatic efficiency at reduced weight flows) can be explained by the increased mass-averaged performance available as a larger percentage of the mass is distributed toward the compressor rotor tip. Besides this effect, however, as the diffusion over the rotor was increased, the work input (enthalpy rise) was increased at the compressor rotor tip section. As pointed out with turning near the axial direction, this could have been obtained only by increased turning in the rotor passage. As reported in reference 4, the tip section obtained a turning of about  $7^\circ$  less than the axial direction at the open-throttle point. Thus, increasing the diffusion over the rotor appears to cause a deterioration of the flow along the rotor hub section and results in improved flow over the rotor tip section, so that some increase in effective turning is obtained. The data indicate an increase in enthalpy rise of about 14 percent as the rotor is throttled from impulse to audible stall. Increasing the turning by these  $7^\circ$  would account for 8 to 10 percentage points of this increase.

#### Stage Considerations for Rotor Performance

The performance characteristics of this compressor rotor component indicate that, as some diffusion is obtained on the rotor, the absolute discharge Mach number can be reduced to about 1.63 (from 1.93 near the impulse

condition) with only a small loss in total-pressure ratio and adiabatic efficiency. This characteristic was not exhibited by the rotors of references 1 to 3. As previously noted, for this rotor the work input would be expected to, and does, remain essentially constant, since the rotor turns to the axial direction; and thus the total-pressure ratio would not vary appreciably with diffusion on the rotor. The efficiency trend, however, must result from the relatively good flow condition over the compressor rotor even when some diffusion is obtained across the rotor.

Previous investigations indicate that stator losses are largely a function of the stator-entrance Mach number. The fact that the best stage-performance point may occur for this rotor at some other than the best rotor-performance point is shown in figure 7. The rotor component total-pressure ratio and adiabatic efficiency are plotted against the absolute discharge Mach number for a rotational speed of 97.5 percent (reproduced from fig. 4(c)). The two performance curves were computed for the stage by applying normal shock recoveries and previously measured stator recoveries (ref. 3). Computed stage-performance values (fig. 7) peak at an intermediate Mach number. A peak efficiency of about 0.75 is obtained at a discharge Mach number of about 1.6 when normal-shock recoveries for the measured inlet Mach number are considered. For the measured losses of a previous investigation, the stage curves peak at an efficiency of 0.64 for a Mach number of about 1.5. Computed total-pressure ratios for these two performance points would be about 4.84 and 4.0, respectively. Peak total-pressure ratios occur at slightly lower Mach numbers than the computed peak adiabatic efficiencies. These curves indicate the gain in performance that may be obtained by increasing the recoveries in the diffusing stators as well as the necessity of matching the rotor and stators at their best operational point. It should be pointed out that these stage curves do not represent operational curves but rather the peak values that may be obtained by matching at the assumed conditions. The data points previously described at very low weight flows (below minimum total-pressure ratio) will not be considered, because they must have been obtained with some flow separation and unsteady flow, and for this reason the flow out of the rotor may not be suitable for efficient diffusion in stators.

### Stage Performance

Performance with stators at design setting angle. - The diffusing stators described were designed to operate approximately at the best computed stage-performance point ( $M_2 = 1.55$ ). The stage total-pressure ratio and adiabatic efficiency for these stators and rotor are shown in figure 8 at 77.9, 87.6, 92.5, and 97.5 percent of design speed. A stage total-pressure ratio of about 4.0 is obtained at an adiabatic efficiency of about 0.66. The weight-flow range for 97.5-percent design speed is between 42 and 44 pounds per second. As the rotational speed is reduced, the range of weight flow is increased, the stage total-pressure ratio is decreased, and the peak stage adiabatic efficiency increases slightly to

1512

CF-2 back

a value of about 0.69 at 77.9-percent design speed. The measured weight flows indicate that the rotor is being operated near the point of minimum total-pressure ratio and adiabatic efficiency (see figs. 4(a) and (b)). Computations of stage efficiency (fig. 7) indicate that the rotor is operating at a Mach number lower than desirable for best stage performance. In this stator design, the flow area through the stators seemed to be large enough, even in the presence of considerable losses. Since the axial-flow component is subsonic, the flow angle approaching the stator blade row would be controlled by the slope of the suction surface of the stator blade along the entrance section (as described in ref. 6). Thus, if this portion of the blade is not parallel to the discharge flow direction from the rotor, an adjustment in the flow will be necessary between the rotor and stators similar to that described in the reference. This adjustment must reach some stable condition where the flow angle out of the rotor, the flow angle set by the stator blades, and the losses and adjustment in the space between the rotor and stators are compatible. This adjustment of the flow probably accounts for some of the difficulty of making measurements in this region and the sometimes apparent change between rotor performance as measured in component and stage investigations even though the same instrumentation is used.

The suction surface of these stators was at an angle greater than the desirable flow from the rotor at the stage design point. Thus, the adjustment would result in a reduction in the axial component ahead of the stators. This, in turn, would cause the rotor to operate with a lower discharge Mach number than that desired for the design point.

Stage performance with stators set at reduced angles. - Previous considerations indicate that improved stage performance might be obtained (improved rotor performance in the stage) if the rotor could be operated at a somewhat higher discharge Mach number. This was attempted in two steps by decreasing the stator blade angles  $3^\circ$  and  $6^\circ$  below the design angle and measuring the change in stage performance. As the stator angles are decreased, the flow area in the stators increases and probably becomes excessive. The length and shape of the entrance section of the stator blades vary as the blades are set to lower angles. Since both the area effect and blade slope tend to match the rotor and stator at a lower rotational speed than design when the stator angles are decreased, only the intermediate-speed data were taken.

The over-all stage data for the reduced stator angles are shown in figure 8 along with the design angle setting. Whereas the stage adiabatic efficiency seems to be somewhat higher for the  $3^\circ$ -reduced stator angle, the range of total-pressure ratio and weight flow seem to be little affected at 77.9 and 87.6 percent of design speed. However, for the  $6^\circ$ -decreased stator angle at 77.9-percent design speed, the equivalent weight flow increased from about 30.5 to about 33.5 pounds per second. At 87.6-percent design speed, the equivalent weight flow increased from

about 39.5 to about 43.1 pounds per second. The stage total-pressure ratios increase only slightly; however, the stage adiabatic efficiency increases from about 0.70 to about 0.77 and from about 0.70 to 0.74 for 77.9 and 87.6 percent of design speed, respectively. Thus, the two best stage-performance points measured for 87.6 and 77.9 percent of design speed would be at a total-pressure ratio of 3.4 and an adiabatic efficiency of 0.74, and at 2.7 and 0.77, respectively. Part of the increase in performance was obtained by moving the rotor to a more favorable operating point. Some improvement in stage performance also may have resulted from a reduction of losses in the stators. Flow conditions over the stators will be considered in the following section.

### Stator Performance

The performance of the stators at the three settings is compared in figure 9, in which stage absolute discharge Mach number is used as the abscissa. The data of figure 9 are for 77.9-percent design speed, where complete data were obtained for each of the three stator angles. The minimum absolute discharge Mach number from the design and the 3°-decreased setting of the stators is about 0.62. When the stator angles were decreased by 6°, however, the discharge Mach number could be reduced only to 0.75 without stage stalling. The reason for this small change in minimum permissible stator-discharge Mach number is not obvious; however, the changes in entrance conditions and area variation through the stators in resetting the blade angles apparently affect the stalling characteristics of the stage.

For the design setting angle of the stators, the equivalent weight flow varied from about 22.5 to about 30.5 pounds per second. In this case, the static-pressure rise could apparently be felt through the stators and thus affected the performance of the rotor. For the 3°-reduced stator blade angle, the equivalent weight flow varied only between 28.05 and 29.95 pounds per second over the entire range of back pressure; for the 6°-reduced setting, the weight flow was almost constant at 33.8 pounds per second. No obvious reason for this effect of stator blade-angle setting on stage weight-flow range can be given.

Reducing stator-discharge angles by 3° results in a peak adiabatic efficiency (0.71) at about the same discharge Mach number as the design setting, and the decrease from this peak value is very gradual. For the setting of the stators 6° below the design angle, the adiabatic efficiency is increased to a value of about 0.78 and remains essentially constant over the range of discharge Mach numbers.

The stage total-pressure-ratio curves for each of the three configurations are also shown in figure 9. The total-pressure ratio at the  $3^\circ$  setting angle is very close to that at the design setting except near the low discharge Mach numbers, when the design setting seems to decrease from the near-constant value of 2.4. However, for the data obtained with the stator angles reduced  $6^\circ$ , the stage total-pressure ratio is increased to about 2.7.

With the measurements taken at instrument stations ahead of and behind the stators, total-pressure recoveries over the stators were computed (fig. 9). For the design and  $3^\circ$ -reduced settings of the stators, the total-pressure recovery is about the same and peaks at a recovery of about 0.87. As the stator angles are decreased by  $6^\circ$  from the design angle, the total-pressure recoveries are increased to about 0.93. Decreasing the stator angles results in improved operation of the stators as well as the rotor. The increased recovery in the stator may be due to the improved flow conditions entering the stators, since the rotor operational point is changed to a more favorable condition.

The stator-entrance Mach number was obtained from the pressure measurements between the rotor and stators (fig. 9). The variation in measured Mach number seems to be about the same for each of the configurations described. The equivalent weight flow varied from about 30 to 34 pounds per second as the stator angles were varied from design setting to  $6^\circ$  less than design. The rotor component data indicate that the absolute rotor-discharge (stator-entrance) Mach number should increase from about 1.23 to about 1.33 over this range of weight flow; the measured values fall within this range (fig. 9). The measurements are probably subject to some error because of the flow adjustment necessary in this region.

The stage performance values for the three stator blade-angle settings were compared at 77.9-percent design speed. The computed best performance point with the assumption of normal-shock recoveries for this speed is shown in figure 10. (This curve is comparable to that for 97.5-percent design speed shown in fig. 7.) The previous section indicates that the discharge Mach number could not be increased above 1.28. Thus, figure 10 indicates that the rotor and stator could not be operated at their best match points, which would be at a Mach number of about 1.4. Several percentage points in stage efficiency and some increase in total-pressure ratio may be obtainable by moving the rotor and stators to this operational point. It can be noted that the computed stage-performance curves at this speed (Mach number range) are relatively flat compared with those at 97.5-percent design speed. Thus, it might be expected that matching the rotor and stators at this intermediate speed would not be as critical as

at the higher rotational speeds. A comparison of the total-pressure recovery obtained with these stators and that obtained with the stators of the investigation of reference 3 is shown in figure 11. The peak total-pressure recovery for the available speeds is plotted against the stator-inlet Mach number along with the curves obtained in the reference and normal-shock recoveries for the given Mach number. Indications are that the total-pressure recovery is improved somewhat over that previously obtained. Also, while reducing the stator angle improved the recoveries somewhat at Mach numbers up to 1.25, at the higher Mach numbers the stators seem to operate equally as well at the design setting. It must be remembered, however, that the design setting points are obtained at a somewhat higher rotational speed. The range of stator-entrance Mach number is rather small, but it does seem to indicate that the total-pressure recovery in these stators may not decrease at the same rate with increasing Mach number as was indicated in the previous investigation.

#### Concluding Remarks

Analysis of the complete performance range of this 16-inch impulse-type supersonic-compressor rotor and the probable stator performance as indicated by previous investigations shows that the best stage performance would be obtained with the rotor operated at some intermediate discharge Mach number rather than the rotor design condition. This best stage performance would probably be obtained at an absolute discharge Mach number of about 1.55 for the design rotor speed. Because of the rapid decrease in rotor performance below this absolute discharge Mach number and because of the rapid increase in stator losses above this Mach number, the matching of the stators and rotor is rather critical. The analysis further indicates that considerable gain in stage performance can be obtained if the total-pressure recovery in the stators can be improved in the range of stator-entrance Mach numbers of 1.4 to about 1.65, since matching the rotor and stators in this range would then allow some improvement in rotor as well as stator performance.

#### SUMMARY OF RESULTS

The 16-inch impulse-type supersonic-compressor rotor with turning to the axial direction was investigated as a single component and as a stage. The rotor design and design performance were reported in part I. In this report, a more complete analysis was made of the rotor component off-design performance, which was necessary to determine how this rotor might be used to best advantage in a compressor stage. A set of diffusing stators was then used with this rotor to investigate the stage performance. The following results were obtained:

1. Considering the range obtained with both discharge annuli, this rotor as a separate component had a very wide range of equivalent weight flow (48.5 to 34.1 lb/sec at 97.5-percent design speed). At 97.5-percent design speed, the adiabatic efficiency was 0.89 at a total-pressure ratio 5.7 and an absolute discharge Mach number of 1.93. This rotor allowed a reduction in Mach number to about 1.65 with a relatively small reduction in adiabatic efficiency and total-pressure ratio. Beyond this point, however, both the adiabatic efficiency and the total-pressure ratio decrease very rapidly.

2. By using the curve of peak total-pressure recovery against stator-inlet Mach number of reference 3 and the rotor component data of this report, a best stage-performance point would be obtained at some intermediate stator-entrance Mach number (1.55 for 97.5-percent design speed). Since there is a rapid decrease in rotor performance at lower discharge Mach numbers and a rapid increase in stator losses at higher Mach numbers, a rather narrow range of computed good stage-performance values resulted.

3. With the stators set at the design angle, the stage total-pressure ratio is about 4.0 and the stage adiabatic efficiency is about 0.66 at 97.5-percent design speed. The range of equivalent weight flow is about 42 to 44 pounds per second, which indicates that the rotor is operating at the point of minimum efficiency and pressure ratio rather than near the point of best stage performance.

4. By adjusting the stators to  $6^\circ$  less than the design setting angle, the stage performance was improved at 77.9-percent design speed from a stage total-pressure ratio of 2.5 to 2.7 and a stage adiabatic efficiency of 0.70 to 0.77. A  $3^\circ$  reduction in stator angle seemed to have a relatively small effect. This gain in stage performance resulted because of improved rotor performance as well as improved stator performance. At 77.9-percent design speed, the total-pressure recovery in the stators increased from about 0.87 to 0.93 as the stator angle was reduced from design angle by  $6^\circ$ .

5. The total-pressure recoveries through these stators are somewhat improved over those of the previous investigation at corresponding Mach numbers. Reducing the stator angle improved the recoveries somewhat up to a Mach number of 1.25; at the higher Mach numbers obtained, however, the stators seem to operate equally well at the design setting.

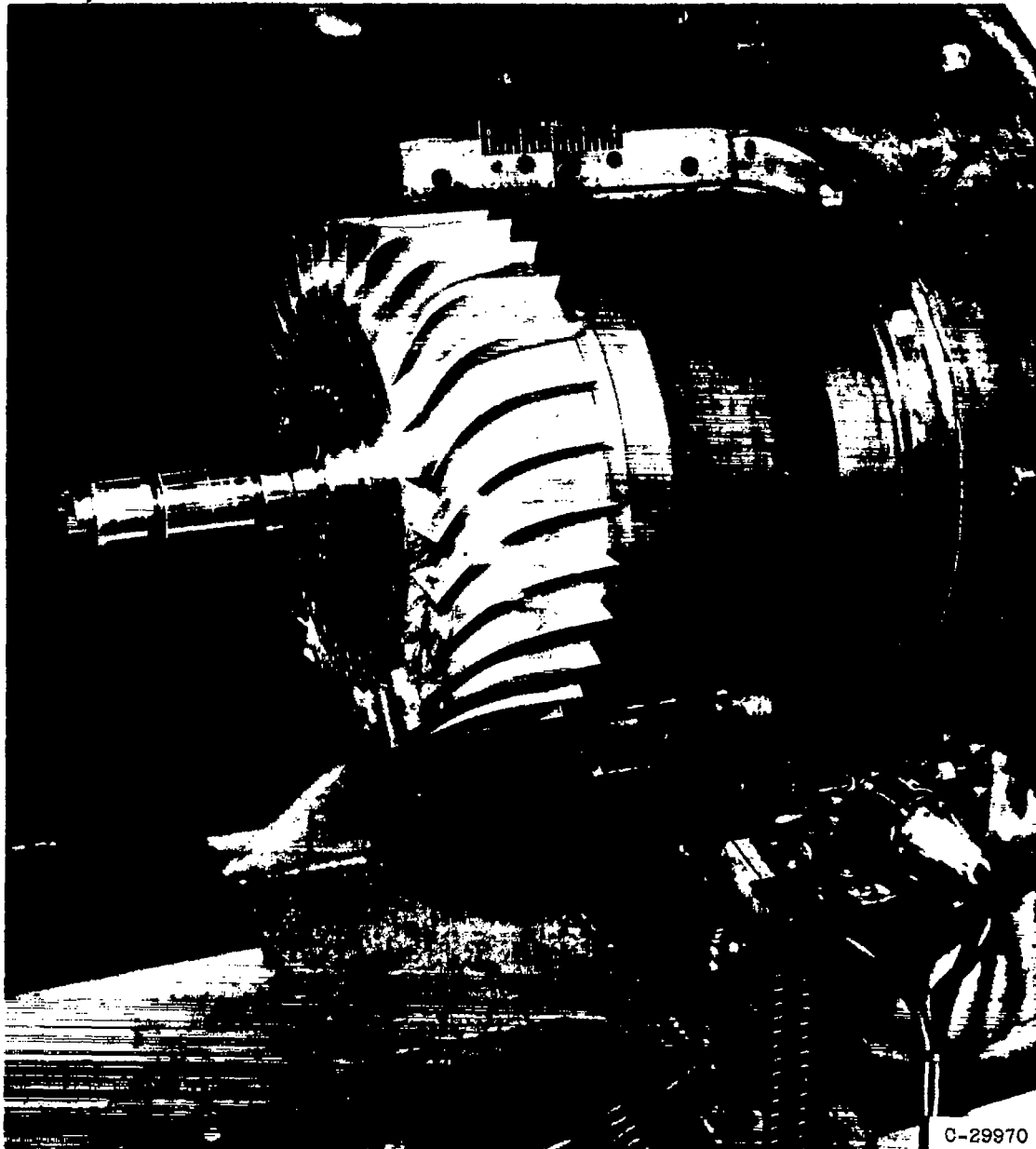
Lewis Flight Propulsion Laboratory  
National Advisory Committee for Aeronautics  
Cleveland, Ohio, December 10, 1953

## REFERENCES

1. Ullman, Guy N., Hartmann, Melvin J., and Tysl, Edward R.: Experimental Investigation of a 16-Inch Impulse-Type Supersonic-Compressor Rotor. NACA RM E51G19, 1951.
2. Goldstein, Arthur W., and Schacht, Ralph L.: Performance of a Swept Leading Edge Rotor of the Supersonic Type with Mixed Flow. NACA RM E52K03, 1953.
3. Jacklitch, John J., Jr., and Hartmann, Melvin J.: Investigation of 16-Inch Impulse-Type Supersonic Compressor Rotor with Turning Past Axial Direction. NACA RM E53D13, 1953.
4. Tysl, Edward R., Klapproth, John F., and Hartmann, Melvin J.: Investigation of a Supersonic-Compressor Rotor with Turning to Axial Direction. I - Rotor Design and Performance. NACA RM E53F23, 1953.
5. Klapproth, John F., Ullman, Guy N., and Tysl, Edward R.: Performance of an Impulse-Type Supersonic Compressor with Stators. NACA RM E52B22, 1952.
6. Kantrowitz, Arthur: The Supersonic Axial-Flow Compressor. NACA Rep. 974, 1950. (Supersedes NACA ACR L6D02.)

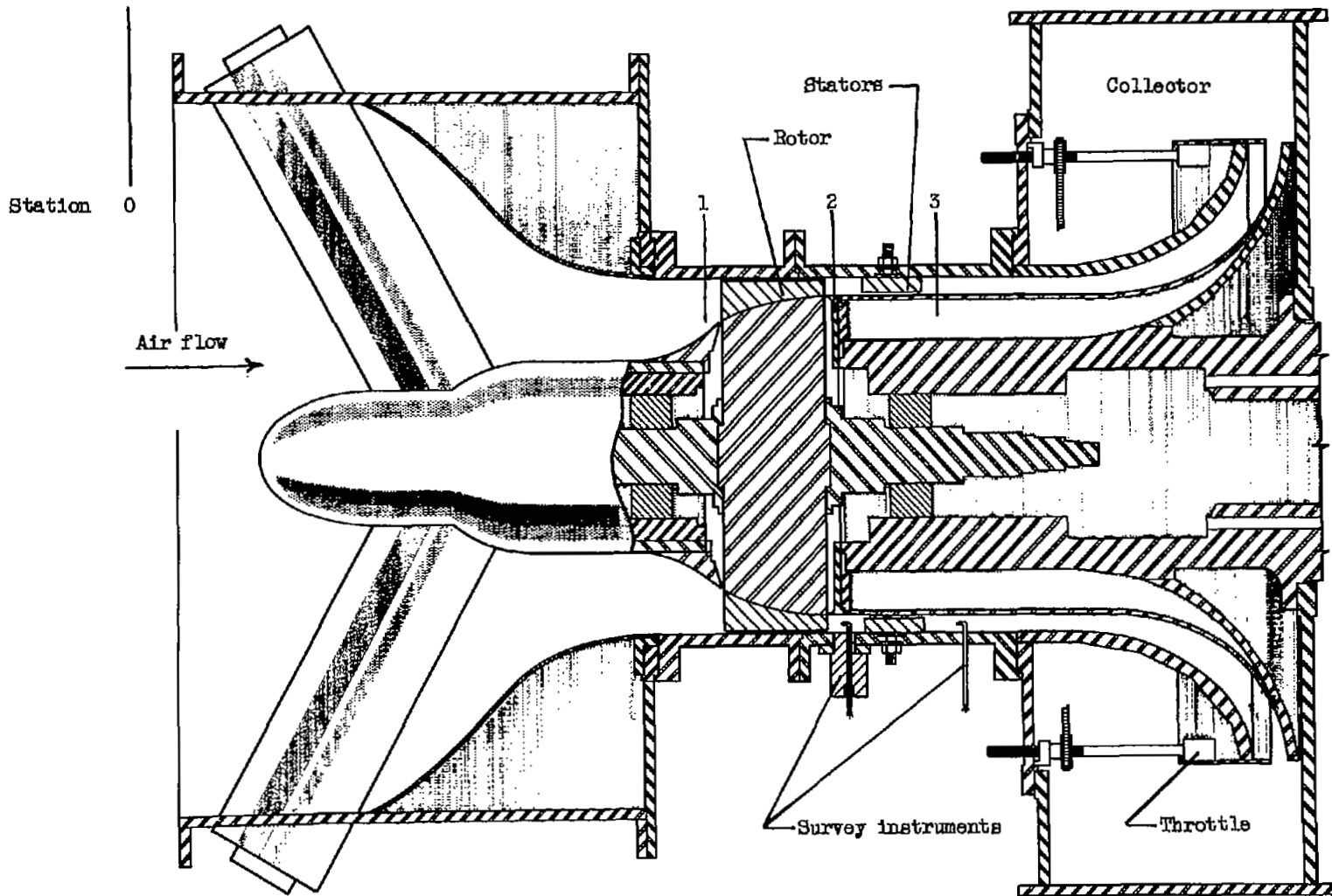
3151

CF-3



(a) Rotor installation.

Figure 1. - 16-Inch impulse-type supersonic-compressor rotor installed in variable-component test rig.



(b) Schematic diagram, showing diffusing stators and instrumentation stations.

CD-3392

Figure 1. - Concluded. 16-Inch impulse-type supersonic-compressor rotor installed in variable-component test rig.



C-29877

Figure 2. - Stators used in stage investigation of supersonic-compressor rotor with turning to axial direction.

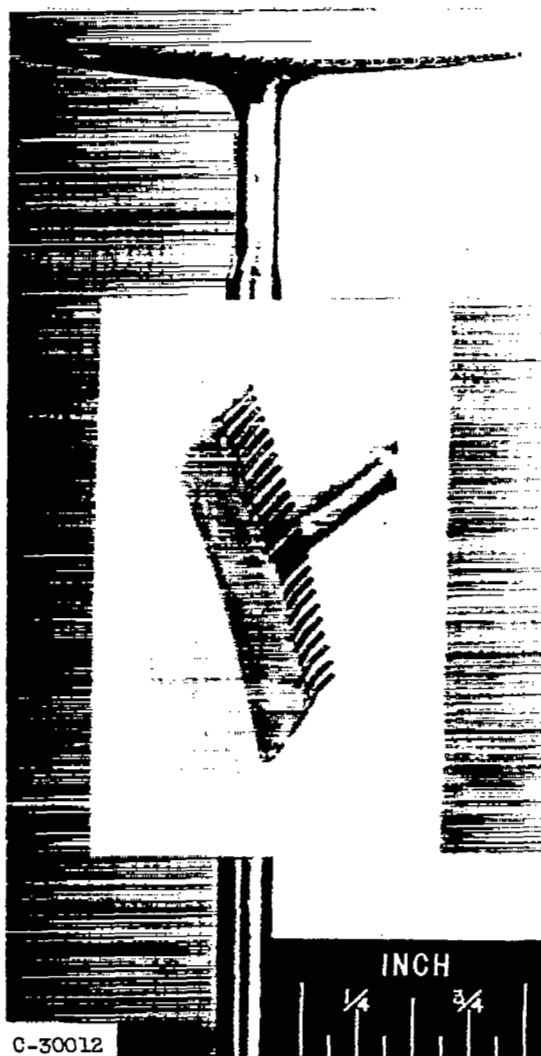
3151



C-31523



Stagnation-type  
thermocouple probe



C-30012

24-Tube total-pressure rake

Claw-type total-  
pressure probe

Stagnation-type  
thermocouple probe

Figure 3. - Instruments used in stage investigation of supersonic-compressor rotor with turning to axial direction.

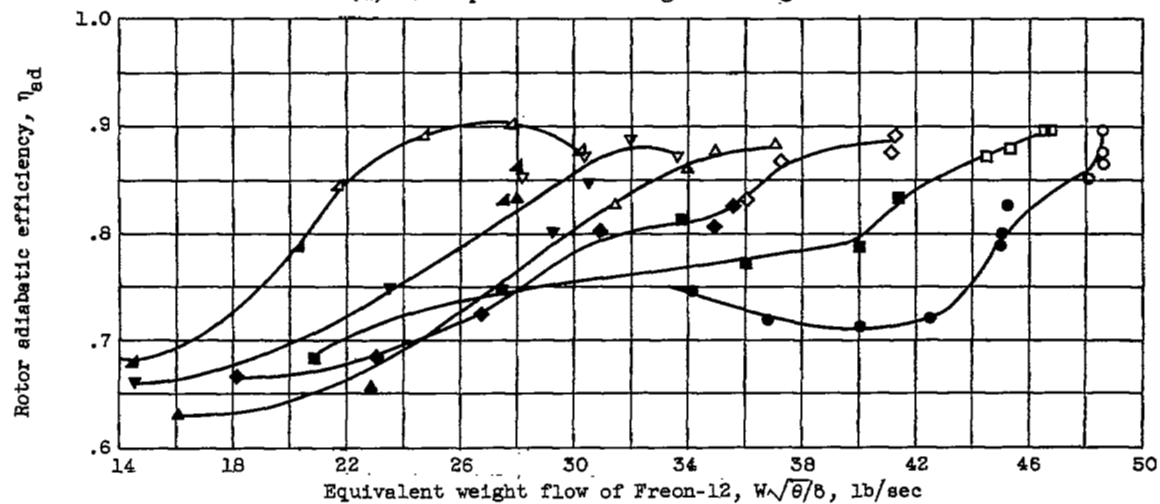
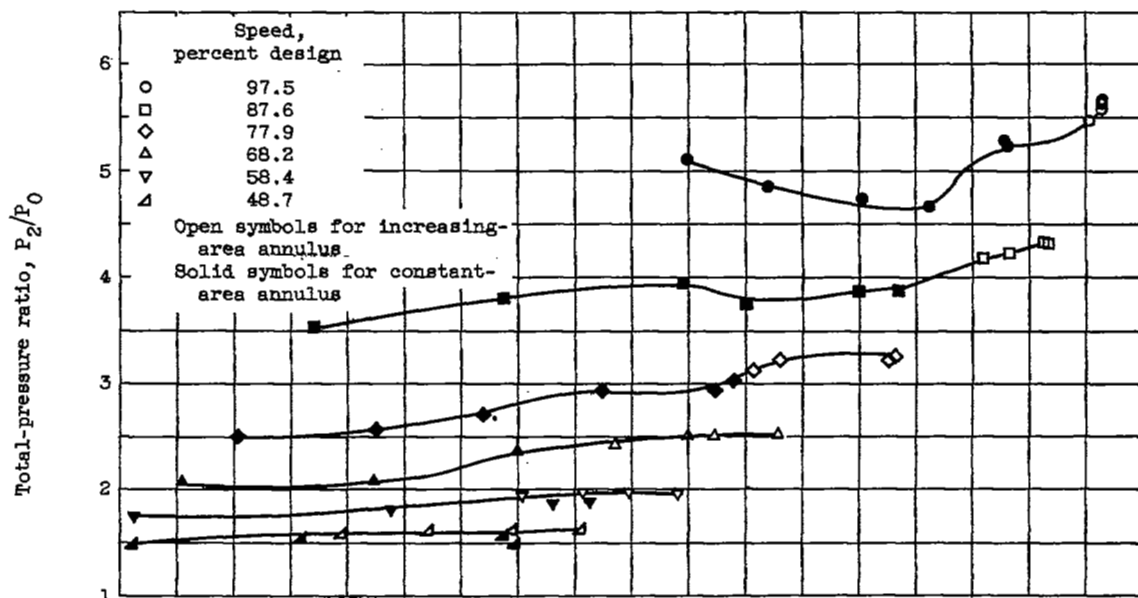
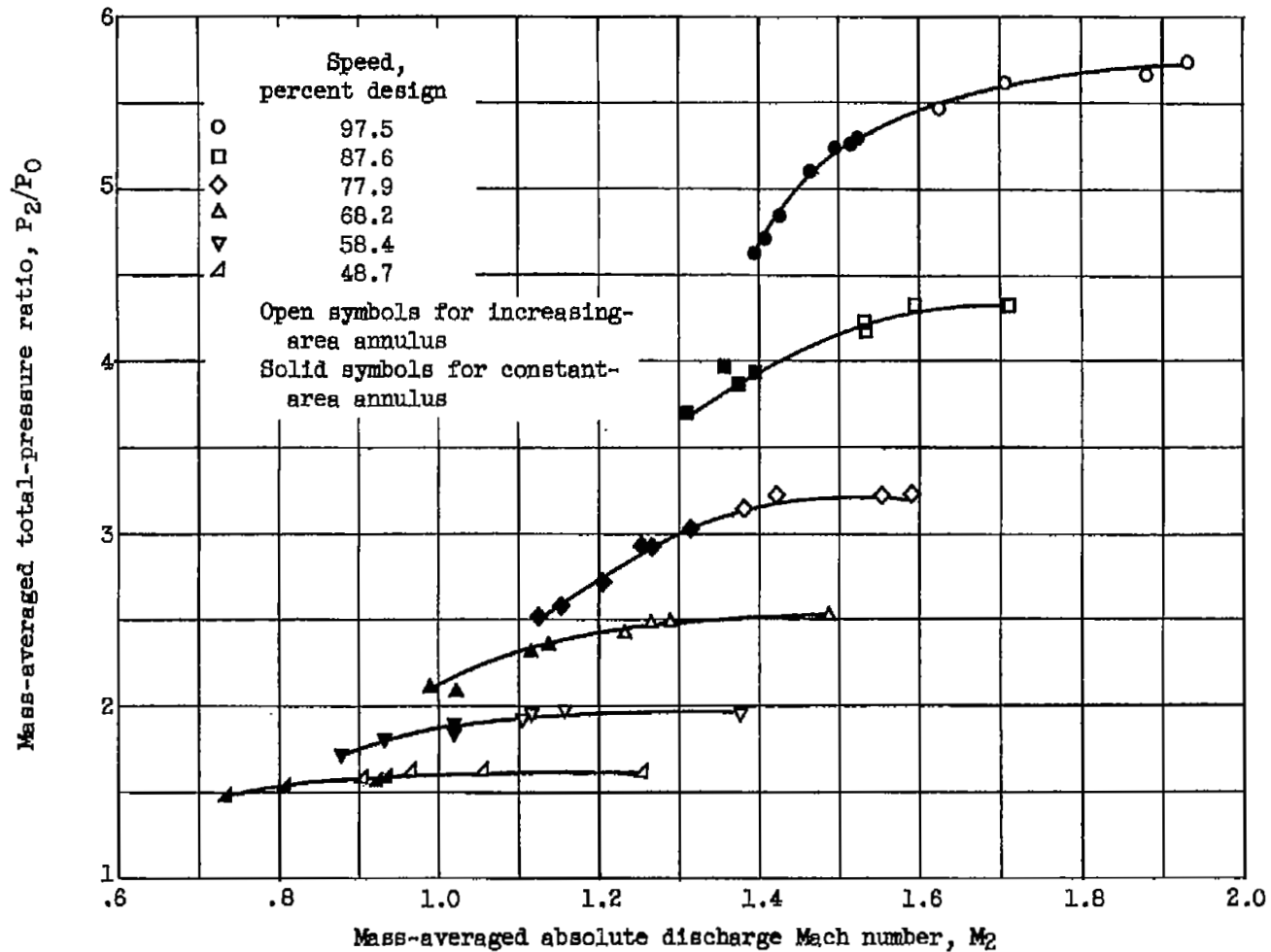
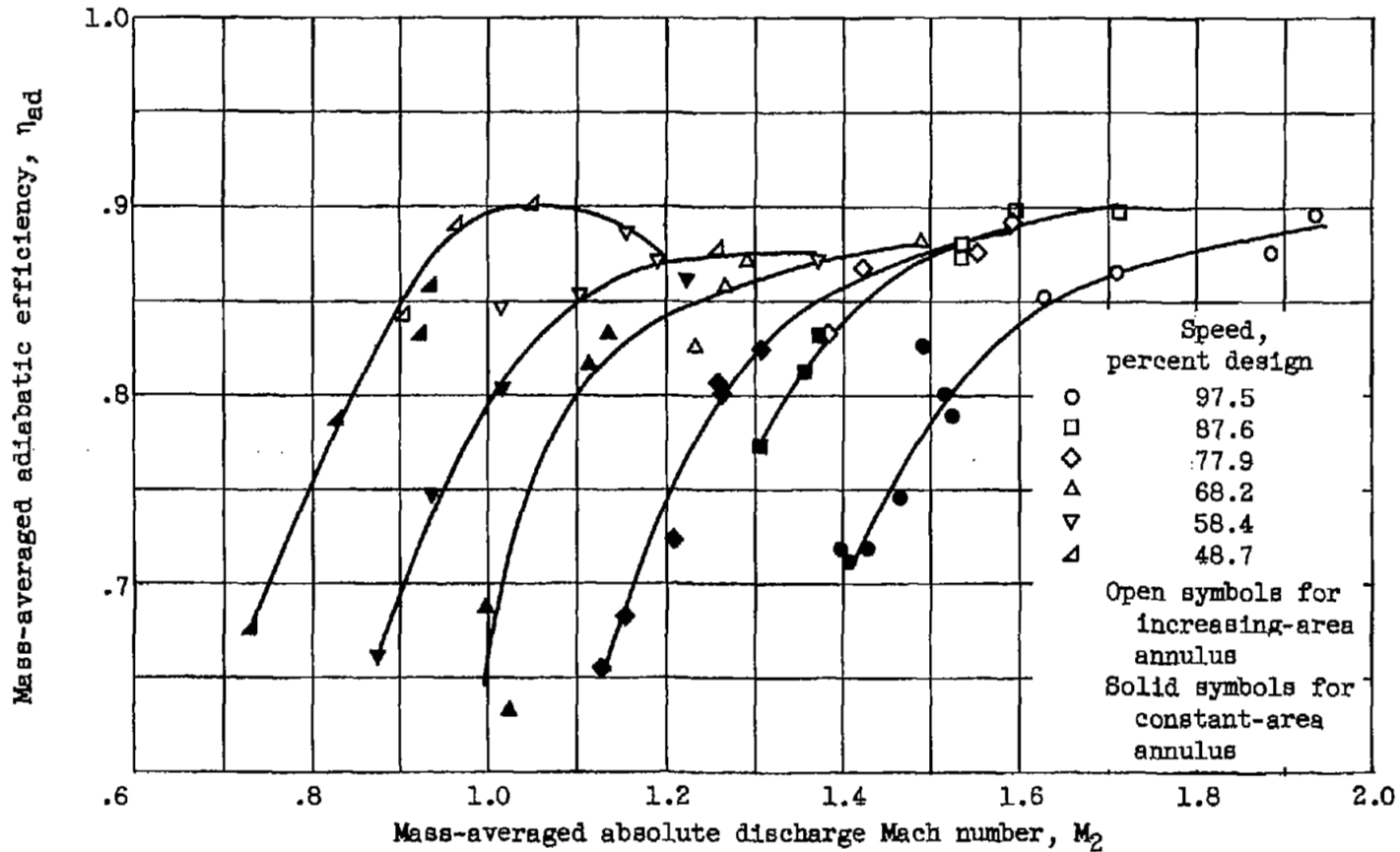


Figure 4. - Performance characteristics of 16-inch impulse-type supersonic-compressor rotor with turning to axial direction.



(c) Mass-averaged total-pressure ratio against absolute discharge Mach number.

Figure 4. - Continued. Performance characteristics of 16-inch impulse-type supersonic-compressor rotor with turning to axial direction.



(d) Mass-averaged adiabatic efficiency against absolute discharge Mach number.

Figure 4. - Concluded. Performance characteristics of 16-inch impulse-type supersonic-compressor rotor with turning to axial direction.

3151

CF-4

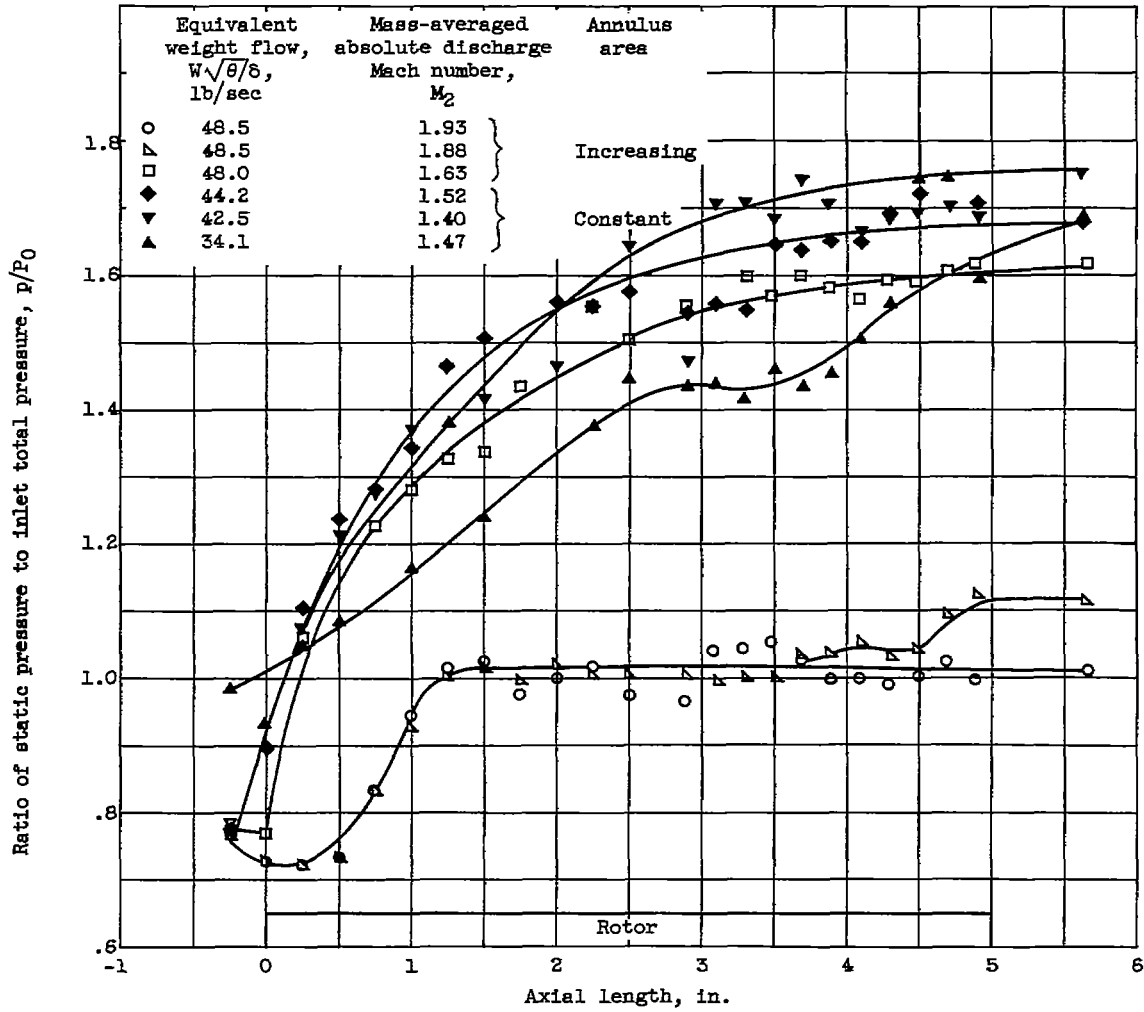


Figure 5. - Static-pressure profile over 16-inch impulse-type supersonic-compressor rotor with turning to axial direction. Speed, 97.5-percent design.



3151

CF-4 back

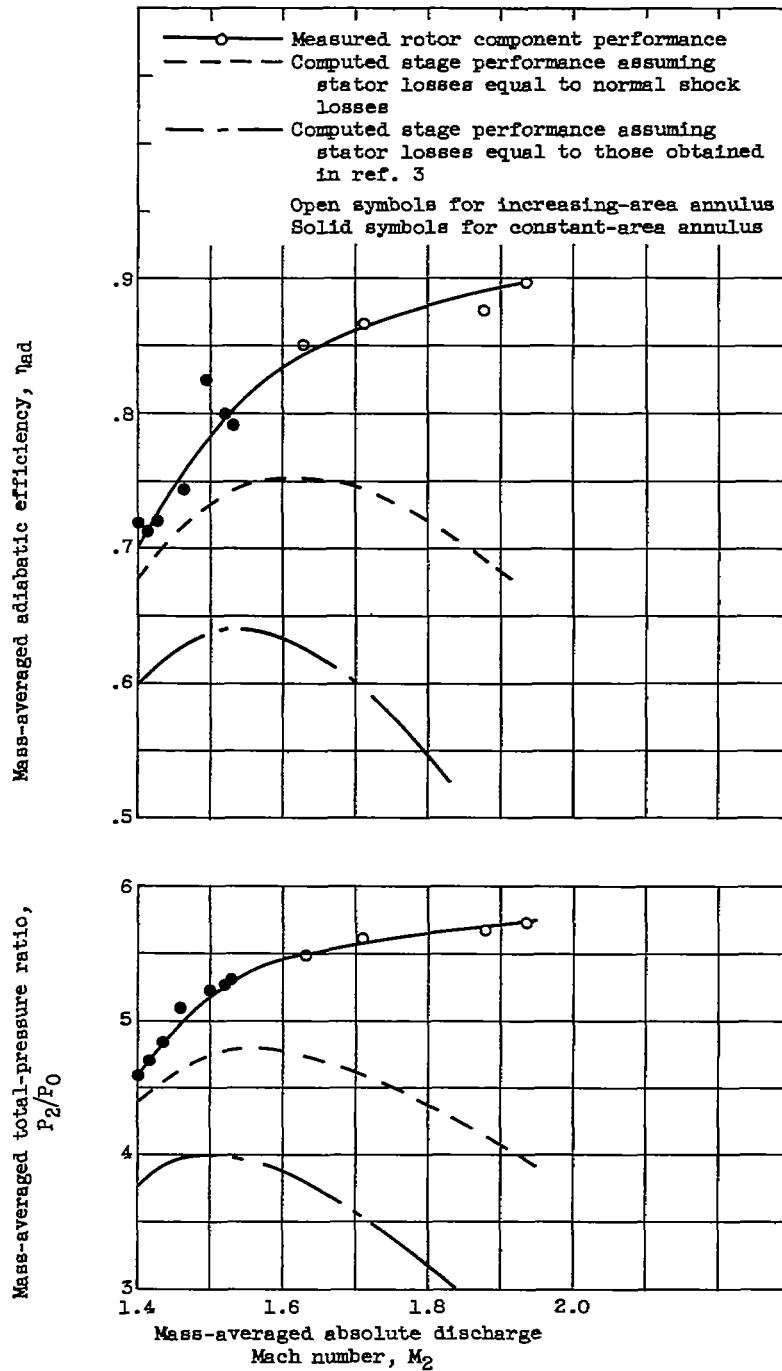
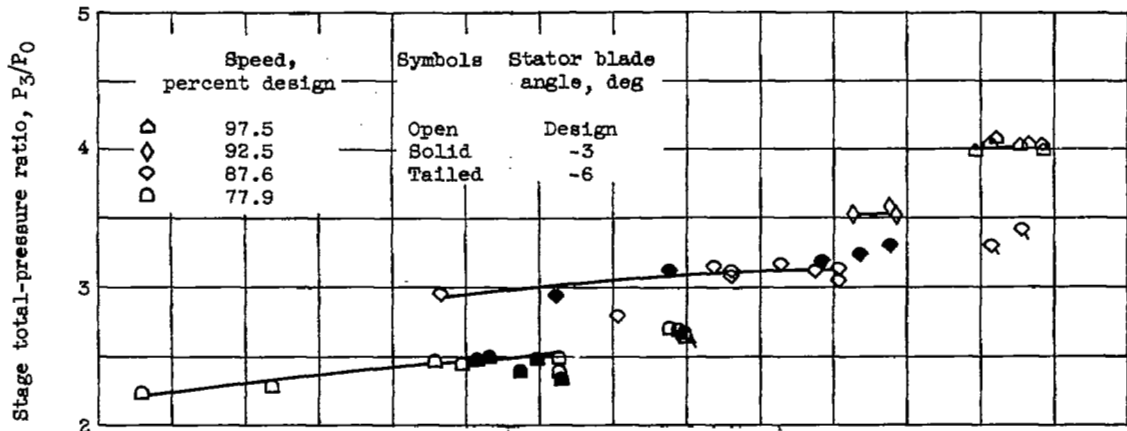
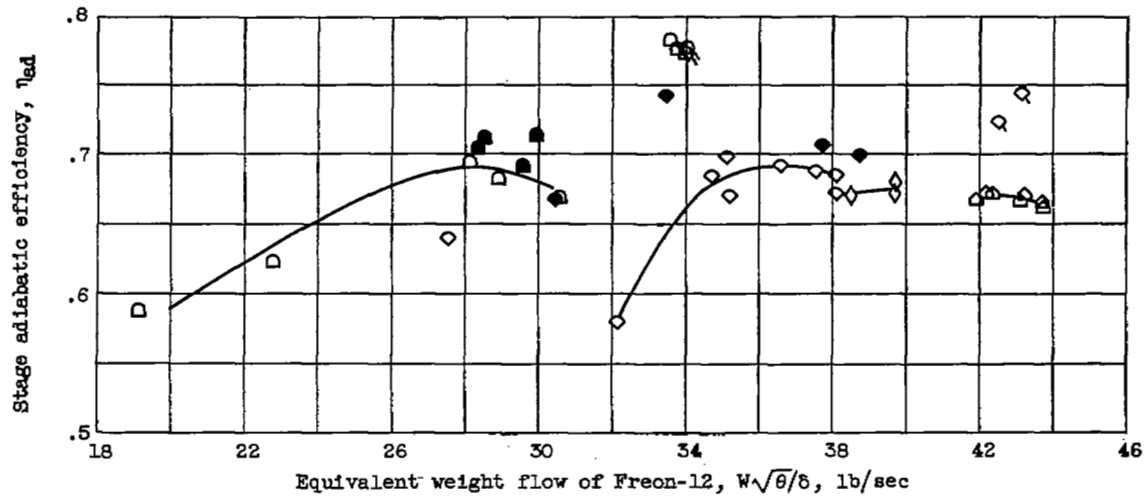


Figure 7. - Computed stage performance for 16-inch impulse-type supersonic compressor. Speed, 97.5-percent design.



(a) Total-pressure ratio.



(b) Adiabatic efficiency.

Figure 8. - Stage characteristics of 16-inch impulse-type supersonic-compressor rotor with diffusing stators.

3151

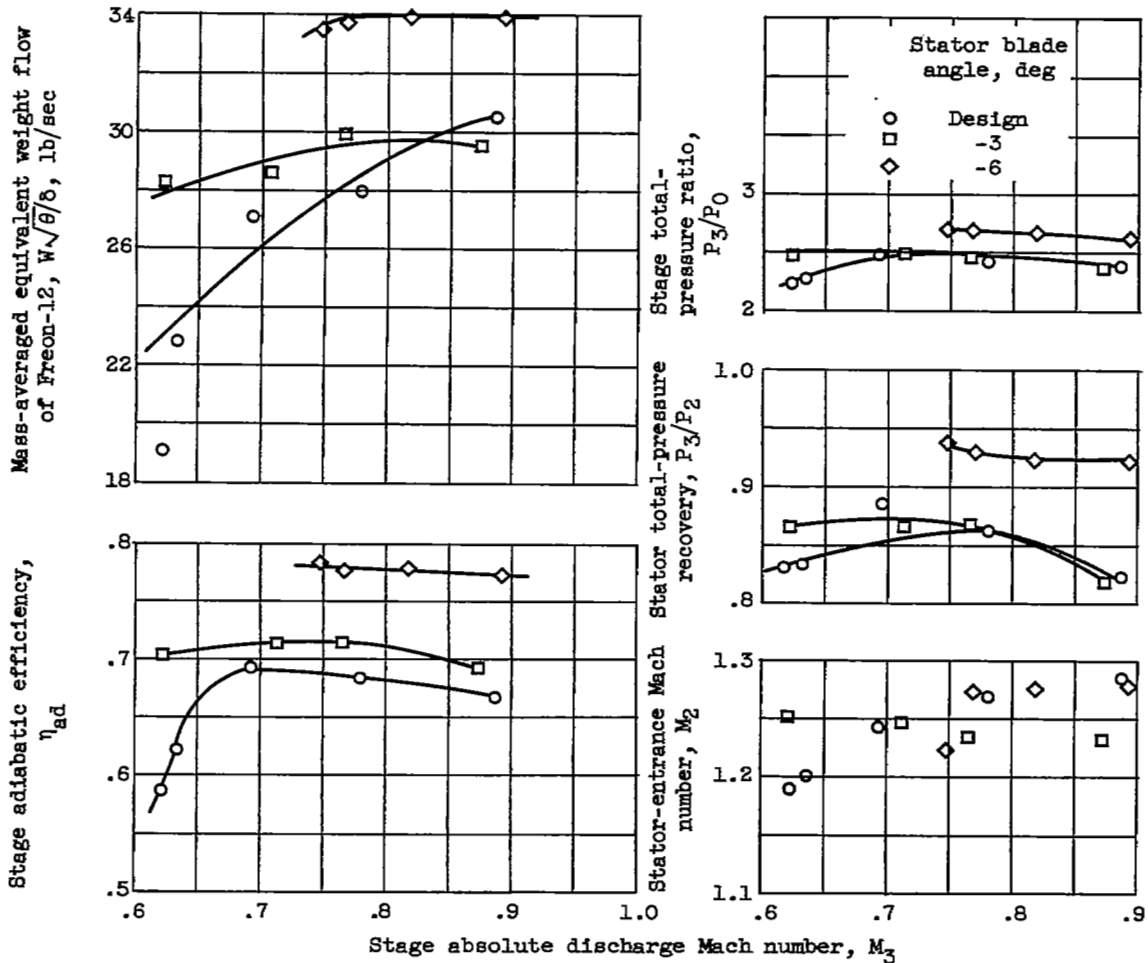


Figure 9. - Variation of performance parameters at stator discharge for 77.9-percent design speed.

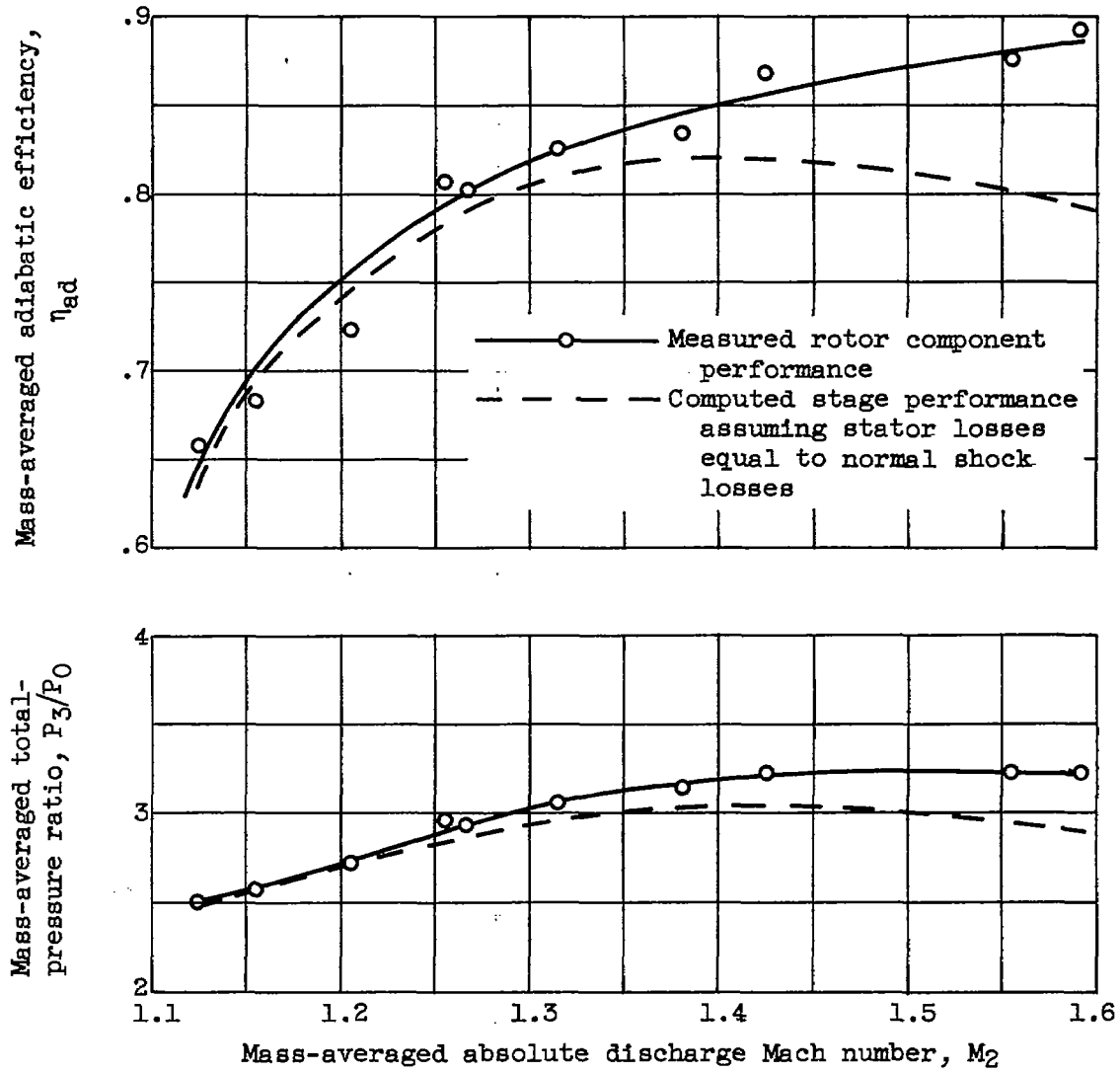


Figure 10. - Computed stage performance for 16-inch impulse-type supersonic compressor. Speed, 77.9-percent design.

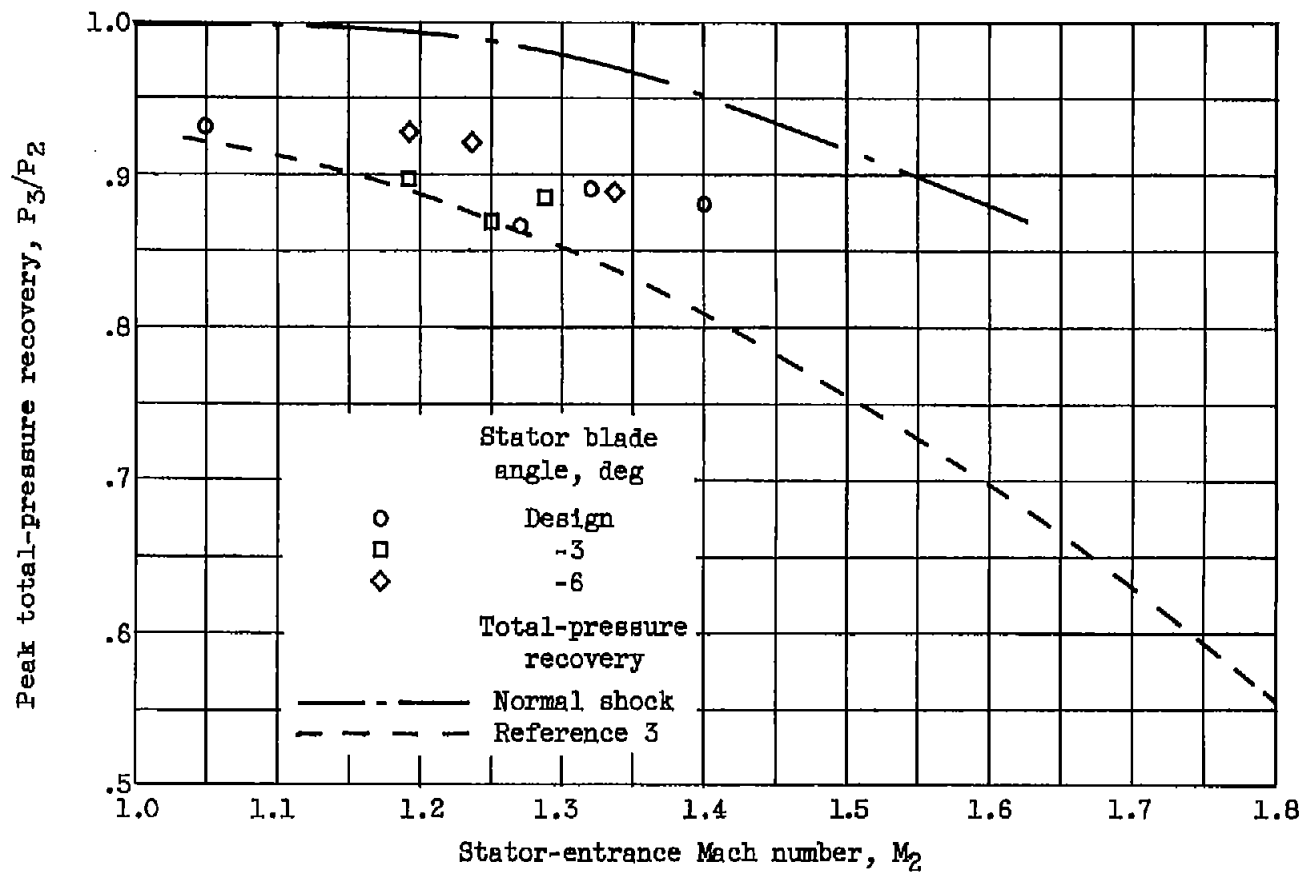


Figure 11. - Peak total-pressure recovery over stators when installed behind 16-inch supersonic-compressor rotor with turning to axial direction.

NASA Technical Library



3 1176 01435 3305

